



Applicability of blocking laws in non-Newtonian fluid membrane filtration

Gema Sakti Raspati*, TorOve Leiknes

Department of Hydraulic and Environmental Engineering, Norwegian University of Science and Technology, S.P. Andersensvei 5, Trondheim 7491, Norway

Tel. +47 735 94746; Fax: +47 735 91298; email: gema.s.raspati@ntnu.no

Received 2 August 2013; Accepted 1 February 2014

ABSTRACT

The blocking laws for constant flux non-Newtonian fluid filtration were derived by means of the Rabinowitsch–Mooney equation in the form of different first-order derivative expressions of pressure change over filtered volume dP/dV . The modified blocking laws were found theoretically sound as the modified equations reduced to those of classical blocking laws if the value of flow behavior index of Newtonian fluid was inserted. Dead end, constant flux microfiltration experiments of kaolin, titanium oxide (TiO_2), and sodium carboxymethyl cellulose at different concentrations (0.25–2% w/v) and at different fluxes (80 and 120 L/m²/h) were conducted to investigate the impact of non-Newtonian fluid behavior due to particle dispersion in water and soluble material on membrane filtration. It was found that the rheology of the fluid changed due to material retention on the membrane which led to conclusion that the model was not fully confirmed and, thus, its applicability might be insufficient to elucidate fouling mechanisms in constant flux, non-Newtonian fluid filtration.

Keywords: Blocking laws; Rheology; Constant flux; Non-Newtonian fluid; Membrane filtration

1. Introduction

Rheology has become an established subject to characterize deformation and flow of materials in response to stress. The tribute to such knowledge is not only ancient science, but has also been the research focus of distinguished scientists and Nobel laureates [1]. According to rheology, fluids with viscous behavior are generally divided into two groups, Newtonian and non-Newtonian, where the latter can be further subdivided into time-independent and time-dependent fluids. A non-Newtonian fluid is defined as any fluid that does not obey Newton's law

of viscosity [1–3]. At constant temperature and different shear rates, the stress components (i.e. shear stresses) that operate at a point in the fluid body are directionally dependent (anisotropic). Fluids of simple structure, e.g. water, gases, mixtures of small organic/inorganic molecules, are considered Newtonian. Fluids with more complex composition and structure are usually non-Newtonian, for example, solutions of macromolecules and multiphase fluids (e.g. emulsions and solid suspensions). Water and wastewater treatment installations may, in fact, cope with non-Newtonian fluids in some operational components as fluids exert non-Newtonian behavior if certain conditions are met [4–6]. Rheological properties of Newtonian and

*Corresponding author.

time-independent non-Newtonian fluids can be generalized by the following equation:

$$f(\tau) = \left(\frac{\tau - \tau_0}{K}\right)^{\frac{1}{N}} \quad (1)$$

where K [$\text{kg s}^N/\text{m}^2$] is the consistency coefficient or fluid viscosity, N [-] is the flow behavior index, $f(\tau)[\text{s}^{-1}]$ is the shear rate as a function of shear stress, τ and τ_0 [Pa] are shear stress and yield stress, respectively. The focal point of rheology discussion lies in the values of constant N and τ_0 , given that the value of K for all types of fluids is always larger than zero. Table 1 summarizes fluid classification based on the parameter values in Eq. (1) and an illustration of various time-independent non-Newtonian fluids behavior is given in Fig. 1.

Membrane fouling mechanisms can be explained by many models that have been established i.e. concentration polarization model [7], osmotic pressure and gel layer model [8,9], cake filtration [10,11], and blocking laws [12,13]. Subsequent models have further been derived taking into account fouling mechanism transitions, e.g. transition from concentration polarization to cake formation [14] or transition from pore blocking to cake filtration [15]. For low-pressure membrane filtration systems (i.e. micro-/ultrafiltration), under conditions where the size of particles in the feed-water are smaller or in the region of the membrane pore size, mechanistic models such as blocking laws are considered more appropriate [16]. The blocking laws were originally derived for constant pressure dead-end filtration where conditions dictated the necessity to incorporate rheological aspects of the fluids in the analysis of membrane fouling by the blocking laws [12,13,17]. Throughout its development, researchers have tried to apply blocking laws to analyze numerous experimental results, even when the process conditions were different from those used for the initial development of the model, as summarized by Hlavacek and Bouchet [18].

Table 1
Summary of fluid types and rheology constants

Fluid type	K	N	τ_0
Newtonian	$0 <$	1	0
Power-law			
Shear-thinning	$0 <$	$0 < N < 1$	0
Shear-thickening	$0 <$	$1 < N < \infty$	0
Bingham plastic	$0 <$	1	$0 <$
Herschel-Bulkley	$0 <$	$0 < N < \infty$	$0 <$

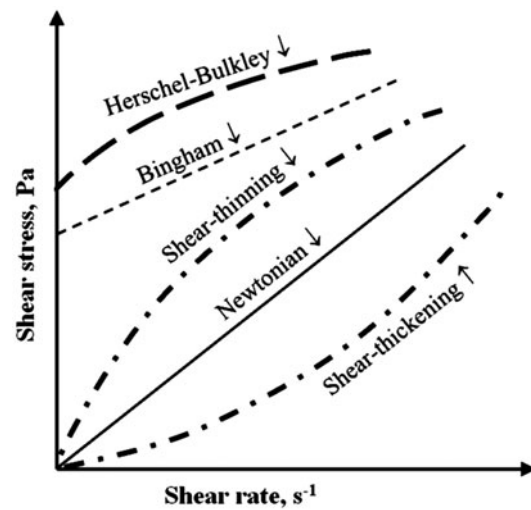


Fig. 1. Typical shear rate vs. shear stress of time-independent fluids [3].

The classical blocking laws for constant pressure membrane filtration discusses four hypothetical types of blocking mechanisms based on the nature of how the materials in the fluid interact with the membranes, resulting in distinct characteristics of permeate flux decrease over time. In contrast, when filtration is based on constant flux operation, the four blocking mechanisms result in a distinct increase of pressure required to maintain the flux. The idealized forms of the physical blocking mechanisms defined by the four hypotheses are illustrated in Fig. 2. The transport of

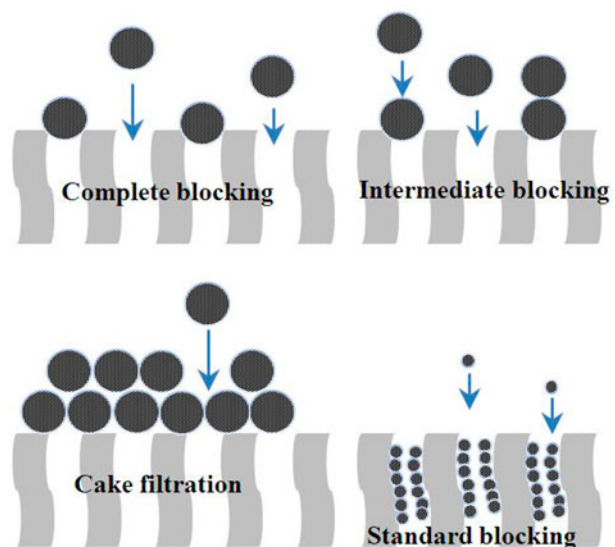


Fig. 2. The four hypothetical forms of membrane fouling in blocking laws.

material to the membrane, however, is under influence of the fluid properties, thus it is necessary to take into account the fluid properties in applying the model in order to be theoretically more precise. A theoretical review on this subject is presented in the first part of this paper, building on the theoretical approach initially done by Shirato et al. [19], and taking into account recent developments of the theory of blocking laws. The aim of this study is to assess the applicability of blocking laws for constant flux membrane filtration, taking into account the impact of fluid rheology on the model parameters, and to assess their applicability in filtration experiments. Results from filtration experiments of non-Newtonian fluid behavior due to high concentration of particle dispersion and non-Newtonian dispersed medium are also presented.

1.1. Theory

The Rabinowitsch–Mooney equation incorporates the shear rate as a function of shear stress in capillary rheology, thus, it gives the possibility to extend basic fluid flow equations (e.g. Hagen–Poiseuille) to various fluids with wide rheological properties (e.g. power-law non-Newtonian, Bingham plastic, or Herschel–Bulkley fluids). The general expression of the Rabinowitsch–Mooney equation is as follows:

$$\frac{u}{r} = \frac{1}{\tau_w^3} \int_0^{\tau_w} \tau^2 \cdot f(\tau) d\tau \quad (2)$$

where u [m/s] represents fluid velocity at radius r [m] which corresponds to shear stress τ [Pa] at the radius and to shear stress at the wall τ_w [Pa]. $f(\tau)$ [s^{-1}] is the shear rate as a function of shear stress. For pressure driven systems, τ_w can be related to pressure P by balancing the forces working along the pores of the membrane,

$$\tau_w = P \cdot r / 2L \quad (3)$$

In this manuscript, the non-Newtonian power-law fluid is characterized by the Oswald–de Waele equation $f(\tau) = (\tau/K)^{1/N}$, which is derived by assigning τ_0 a value of zero in Eq. (1). Thus, integration of Eq. (2) and introducing Eq. (3) yields,

$$u = \frac{N}{3N+1} \left(\frac{P}{2LK} \right)^{1/N} r^{(N+1)/N} \quad (4)$$

Inserting a N value of 1 reduces Eq. (4) to either the Hagen–Poiseuille or the Darcy equation [3]. With

recent development in membrane separation technology, which more commonly use constant flux operation, fouling mechanisms are rather judged by the characteristics of pressure increase as a function of the volume of fluids being filtered [20,21], which corresponds well with the theory of critical volume [22]. Throughout this paper, the derivation of the characteristic equations is presented in the following form,

$$\frac{dP}{dV} = k \cdot P^n \quad (5)$$

where n and k represent the blocking index and blocking constant, respectively. A first-order derivative form is preferred in order to form the characteristic equation for cake filtration which could not be represented by a second-order time derivative form as in the previous study of Hlavacek and Bouchet [18]. For a constant flux system, the following flow balance holds at all times,

$$Q_0 = Q_V \equiv A_0 \cdot u_0 = A_V \cdot u_V \quad (6)$$

where Q [m^3/s] represents total flow of the fluid, A [m^2] is the active membrane surface area, and u [m/s] is the fluid velocity. At any point in this text, the subscripts 0 and V represent the initial condition and condition after a certain amount of filtered volume of each parameter mentioned above. Eq. (6) exemplifies that the reduction of active membrane area due to fouling is compensated by the increase of local pore velocity in the remaining active membrane area in order to produce an equal amount of filtrate. Substituting Eq. (4) to Eq. (6) yields,

$$\begin{aligned} A_0 \cdot \frac{N}{3N+1} \left(\frac{P_0}{2L_0K_0} \right)^{1/N} r_0^{(N+1)/N} \\ = A_V \cdot \frac{N}{3N+1} \left(\frac{P}{2L_VK_V} \right)^{1/N} r_V^{(N+1)/N} \end{aligned} \quad (7)$$

Fouling mechanisms as hypothesized by the blocking laws (Fig. 2) occur under certain assumptions that will be discussed in the following sections. By applying these assumptions to Eq. (7), the formulation of blocking laws in the form of Eq. (5) with different values of blocking index n and blocking constant k that characterize the occurring fouling mechanisms can be obtained. Subscripts CB , IB , SB , and CF following the model parameters are used in this manuscript to represent complete blocking, intermediate blocking, standard blocking, and cake filtration, respectively.

1.2. Complete blocking

The underlying assumption for complete blocking is that every approaching particle will plug a pore completely, resulting in an increase of driving force needed to produce an equal amount of filtrate to compensate a decreasing active filtration surface area on the membrane. Eq. (8) dictates the decrease of active membrane area,

$$A_V = A_0 - \sigma \cdot c_f \cdot V \quad (8)$$

where σ [m²/kg] is the projected particle area normalized to unit mass of the particle, c_f [kg/m³] is the bulk concentration of the particles, and V [m³] is filtered volume. Differentiating Eq. (8) gives the rate of membrane area decrease over filtered volume.

$$\frac{dA_V}{dV} = -\sigma \cdot c_f \quad (9)$$

In complete blocking, there is no change in pore diameter, viscosity or fluid consistency, and the length of the capillary (i.e. r , K , and L are constant throughout the filtration course). Eq. (7) is then reduced to,

$$A_0 \cdot (P_0)^{1/N} = A_V \cdot (P)^{1/N} \Rightarrow P^{1/N} = \frac{P_0^{1/N} \cdot A_0}{A_V} \quad (10)$$

Subsequently, Eq. (10) can be differentiated with respect to volume of fluid being filtered.

$$\frac{dP}{dV} \frac{P^{(1-N)/N}}{N} = -\frac{dA_V}{dV} \left(\frac{P_0^{1/N} \cdot A_0}{A_V^2} \right) \quad (11)$$

By combining Eqs. (9) and (11), the characteristic formula for complete blocking is obtained.

$$\frac{dP}{dV} = N \cdot P_0^{(N-1)/N} k_{CB} \cdot P^{n_{CB}} \quad (12)$$

As seen in Eq. (12), both the blocking index and blocking constant are corrected by the rheology parameter N , where in the case of complete blocking $n_{CB} = (N + 1)/N$ and $k_{CB} = \sigma \cdot c_f / P_0 \cdot A_0$.

1.3. Intermediate blocking

Intermediate blocking was not discussed in the original work on blocking laws for constant flux membrane filtration [23]. In contrast to complete blocking,

intermediate blocking considers the possibility of arriving particles to deposit on the previously attaching layer of particles. It can be proven mathematically that the probability of such a phenomenon is proportional to the active surface area at time t over the initial active membrane surface area (A_t/A_0) in constant pressure system [12]. The same approach was applied in constant flux system e.g. in [21]. Since the ratio of filtered volume over time is constant in constant flux filtration, the probability ratio can be expressed as (A_V/A_0). The rate of reduction of active membrane surface area can then be estimated as follows:

$$\frac{dA_V}{dV} = -\sigma \cdot c_f \cdot \left(\frac{A_V}{A_0} \right) \quad (13)$$

As in the case of complete blocking, in intermediate blocking r , K , and L are constant. Applying these conditions to Eq. (7) will result again in Eq. (11). The only difference between complete blocking and intermediate blocking lies in the characteristic decrease rate of the active membrane surface area in Eq. (13), thus, by substitution the following form is found.

$$\frac{dP}{dV} = N \cdot k_{IB} \cdot P^{n_{IB}} \quad (14)$$

In intermediate blocking only the value of the blocking constant is affected by the rheology, and here $k_{IB} = \sigma \cdot c_f / A_0$ and $n_{IB} = 1$.

1.4. Standard blocking

The principle of standard blocking is defined as a pore-volume reduction due to material deposition/attachment inside the pore structure which eventually reduces the radius of the capillary. Mathematically this is expressed as,

$$N^* \pi (r_0^2 - r_V^2) \cdot L = \frac{c_f \cdot V}{\rho} \quad (15)$$

where N^* [-] is the number of capillaries (i.e. pores), ρ [kg/m³] is the density of the foulant (i.e. particles). The above-mentioned assumption implies K and L in Eq. (7) are constants, but r is no longer constant and, thus, we have to find another expression relating P and r . For standard blocking, Eq. (7) reduces to the following form.

$$\left(\frac{r_0}{r_V} \right)^{1+3N} = \frac{P}{P_0} \quad (16)$$

Inserting Eq. (16) into Eq. (15) results in the following form of equation,

$$1 - \left(\frac{P_0}{P}\right)^{\frac{2}{(1+3N)}} = \frac{c_f V}{N^* \pi r_0^2 L \rho} \quad (17)$$

Given that $N^* \pi r_0^2 = A_0$ and differentiating with respect to pressure and volume, Eq. (17) results in:

$$\frac{dP}{dV} = \frac{(1+3N)}{4} \cdot (P_0)^{\frac{(3N-3)}{(2+6N)}} \cdot k_{SB} \cdot P^{n_{SB}} \quad (18)$$

As in the case of complete blocking, the values of blocking index and blocking constant are heavily affected by the rheology. Eq. (18) shows that for standard blocking $n_{SB} = (3+3N)/(1+3N)$ and $k_{SB} = 2 \cdot c_f / (\sqrt{P_0} \cdot A_0 \cdot L \rho)$.

1.5. Cake filtration

The underlining assumption of cake filtration holds if the increase of driving force is not due to reduction of active surface area for filtration, but rather due to the increase of layer thickness of the retained particles. Modifying Eq. (7) and taking into consideration that A , r , and K are all constants, the relationship for cake filtration is expressed as:

$$\frac{P_0}{L_0} = \frac{P}{L_V} \quad (19)$$

The amount of resistance generated by the clean membrane (R_m) [m^{-1}] is proportional to the length of the capillary i.e. the thickness of the clean membrane L_0 [m] before any deposition of a cake layer. As filtration proceeds the length of “capillary” increases to L_V [m], which can be expressed as $L_V = L_0 + L$. It is apparent that the increase in capillary length L is directly proportional to an increasing thickness of a cake layer and the added hydraulic resistance generated by the cake layer (R_c) [m^{-1}]. The resistance in series model can thus be applied for the cake filtration hypothesis, consisting terms R_m and R_c . Inserting these premises to Eq. (19) yields:

$$\frac{P_0}{R_m} = \frac{P}{R_m + R_c} \Rightarrow P = \frac{P_0(R_m + R_c)}{R_m} \quad (20)$$

However, a more refined definition of cake layer resistance is needed. The amount of resistance generated by a cake is related to inherent properties of the

material that makes up the cake, expressed as \hat{R}_c [m/kg]. For a solution with a bulk concentration c_f of incompressible cake material, the magnitude of the cake layer resistance can be estimated by:

$$R_c = \hat{R}_c \frac{c_f \cdot V}{A_0} \quad (21)$$

Substituting Eq. (21) into Eq. (20) gives:

$$P = P_0 + P_0 \frac{\hat{R}_c \cdot c_f \cdot V}{R_m \cdot A_0} \quad (22)$$

The characteristic equation of cake filtration for Newtonian fluids can then be obtained from the derivation of Eq. (22).

$$\frac{dP}{dV} = \frac{P_0 c_f \hat{R}_c}{A_0 R_m} \Rightarrow \frac{dP}{dV} = k_{CF} \cdot P^{n_{CF}} \quad (23)$$

As seen in Eq. (23), blocking laws predict a linear increase of dP/dV and both blocking index and blocking constant are unaffected by rheology. In the case of cake filtration $k_{CF} = P_0 c_f / A_0 \cdot \hat{R}_c / R_m$ and $n_{CF} = 0$.

Table 2 summarizes the blocking constants and indices of both Newtonian and non-Newtonian fluids. The values of n and k for Newtonian fluids are taken from Huang and co-workers [21] without normalization. The values of n and k of non-Newtonian fluids are heavily modified by the value of N , however, these values conveniently reduce to the values of n and k of Newtonian fluids simply by inserting N value of 1. Derivation of blocking laws for constant flux and constant pressure filtration involves the same set of assumptions for either pore types of fouling (complete, intermediate, and standard blocking) or surface type of fouling (cake filtration). However, the impact of rheology on the model parameters (blocking indices and blocking constant) of the two modes of operation is essentially different. This can be attributed to the fact that the two modes of operation depend on different variables being modeled. Constant pressure filtration depends on the change of the filtration flux while constant flux filtration depends on the change of pressure. Rheology parameters as summarized in Eq. (4) will affect the two filtration variables. However, if one of the filtration variables is set constant then rheology will only impact the other. Consequently, model parameters that depend on either one of the two filtration variables will then be affected by rheology. For the sake of comparison, one may refer to

Table 2
Summary of blocking indices and blocking constants for the blocking laws

	Newtonian fluid ^a		Non-Newtonian power-law fluid	
	n	k	n	k
Complete blocking (CB)	2	$\frac{\sigma \cdot c_f}{P_o \cdot A_o}$	$\frac{N+1}{N}$	$N \cdot \frac{\sigma \cdot c_f}{P_o^{1/N} \cdot A_o}$
Intermediate blocking (IB)	1	$\frac{\sigma \cdot c_f}{A_o}$	1	$N \cdot \frac{\sigma \cdot c_f}{A_o}$
Standard blocking (SB)	3/2	$\frac{2 \cdot c_f}{\sqrt{P_o} \cdot A_o \cdot L \rho}$	$\frac{(3+3N)}{(1+3N)}$	$\frac{(1+3N)}{2} \cdot \frac{c_f}{A_o L \rho} \cdot \left(\frac{1}{P_o}\right)^{\frac{2}{(1+3N)}}$
Cake filtration (CF)	0	$\frac{P_o c_f \cdot R_c}{A_o \cdot R_m}$	0	$\frac{P_o c_f \cdot R_c}{A_o \cdot R_m}$

Note: ^aAdapted from Huang et al. [21].

blocking laws of constant pressure for non-Newtonian fluid filtration as derived by Hermia [12]. The two model parameters in standard blocking and cake filtration are affected by rheology and only the blocking constant is affected in the case of complete blocking. For intermediate blocking, the model parameters are the same as those of a Newtonian fluid. The reason is as explained above, the parameters that are dependent on the variable being modeled will be affected by rheology (e.g. in this case the filtration flow rate). Following this argument, in constant flux filtration only the model parameters in cake filtration that are not dependent on pressure will thus result in the same filtration characteristics for Newtonian and non-Newtonian fluids.

It is necessary to point out that such a derivation of blocking laws does not take into account the more complex phenomena such as changes in the structure of the membrane or deposited particles. The focus of this study has been to apply blocking laws for constant flux non-Newtonian fluid filtration to experimental data using non-Newtonian fluids made up by particle (kaolin and TiO₂) and polymer (sodium carboxymethyl cellulose) dispersions and to assess the applicability in describing fouling mechanisms observed.

2. Materials and methods

2.1. Membranes and feed solution

Experiments were conducted with a filtration unit using a Sartorius' cellulose nitrate microfiltration membrane with a nominal pore size of 0.8 μm and total membrane area of 13.86 cm². The same type of membrane was used in all filtration experiments, with a new membrane used for each experiment. The membranes were pre-conditioned prior to filtration experiments by soaking them in deionized water of same pH and ionic strength as the feedwater for 1 h, and then conducting the filtration experiment for 30 min at the set flux of the experimental plan. Dispersions of

model particles were prepared by adding titanium oxide TiO₂ AEROXIDE[®] P25 (Evonik Degussa) (0.5, 1, and 2% w/v), commercial laboratory-grade kaolin (Prolabo) (0.5 and 1% w/v), or sodium carboxymethyl cellulose (CMC, Sigma-Aldrich) (0.25% w/v) into deionized water (Milli-Q Millipore). Ionic strength was adjusted by adding NaCl and pH by adding NaOH. The fluids were then subjected to ultrasonic bath (SANPA W-115/118 Honda Electronics) where a frequency sequence of 28, 45, and 100 Hz were subsequently applied for 4 min. All experiments in this study were conducted with an ionic strength of 10⁻³ mol/L and pH of 9.

2.2. Analytical methods

Particle sizing was done using an instrument based on light scattering techniques (LS230 Beckman-Coulter) and rheology tests were conducted using a double-gap cell (DG-27) in a rheometer Physica MCR-301 (Anton-Paar) at constant temperature of 20°C over a shear rate range of 1–1500 s⁻¹. The pH of the feed solutions was measured by SympHony SP70P (VWR).

2.3. Setup of filtration experiment

A series of dead-end constant flux filtration experiments were conducted in an unstirred bench scale membrane test cell (Fig. 3). Feed water and permeate suction were achieved by peristaltic pumps (Masterflex L/S Cole-Parmer) and the amount of permeate was monitored by measuring the weight of permeate (E1500D OHAUS) over time on a balance. The data from temperature (SEM203 Status Instrument) and pressure transducers (EW-68075-02 Cole-Parmer) were recorded by using the data acquisition system LabVIEW 2010 software (National Instruments). All filtration experiments were conducted at a constant water temperature of 20°C with a variation of water temperature within ±1°C.

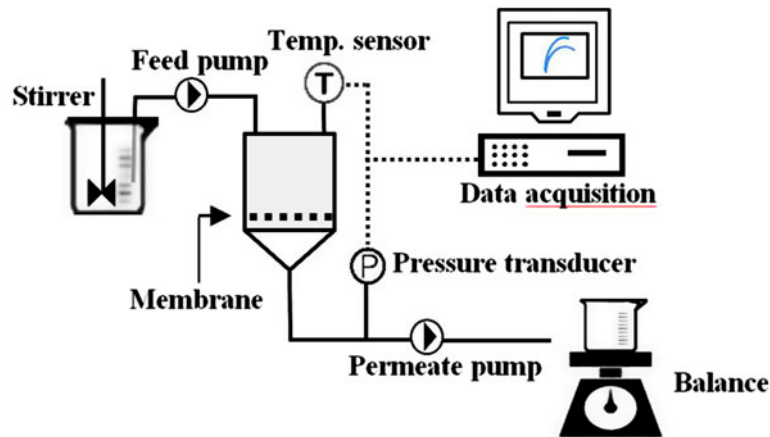


Fig. 3. Schematic diagram of the dead-end filtration system used in the study.

3. Results and discussion

3.1. Rheology of the feed solutions

Fig. 4 shows the rheograms of the materials used in this study (0.5, 1, and 2% w/v kaolin and TiO_2 , 0.25% w/v CMC) at 20 °C and the lines represent fittings using Eq. (1). Kaolin and TiO_2 were aimed to represent non-Newtonian fluid behavior due to particle dispersions in water, while CMC should be able to dissolve in the water and change the medium to be non-Newtonian.

Kaolin dispersions for the two concentrations investigated showed characteristic Newtonian fluid properties with N values of around 1 (1.009 and

0.9994 for 0.5 and 1% w/v, respectively). In contrast, TiO_2 solutions investigated showed characteristics of power law fluids, where the concentrations of 0.5 and 2% w/v displayed shear-thinning fluid properties (N values of 0.9669 and 0.927, respectively) and shear-thickening fluid properties at 1% w/v (N value 1.03). The fact that TiO_2 exhibits different fluid behavior, especially at 1% w/v, was also reported by Santillán and co-workers [24] where TiO_2 -acetyl acetone dispersions were characterized in a range of 0.3–2.5% w/v over a shear rate range of 10–250 s^{-1} . TiO_2 was reported to behave as a shear-thickening fluid at 1% w/v while it behaves like a shear-thinning fluid at any other of the concentrations studied. Unfortunately,

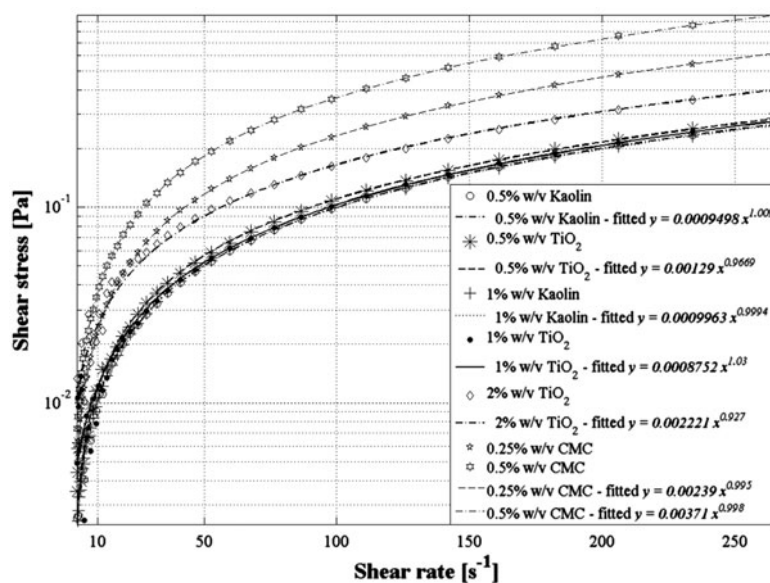


Fig. 4. Rheology measurements of the feed solutions.

the authors did not elaborate the issue further as to why such a phenomenon arises. However, the conditions reported were the basis for choosing the test conditions in this study enabling investigating the two different power law fluid behaviors (i.e. shear-thinning/shear-thickening). CMC behaved like a shear-thinning fluid with N value of 0.995.

One may argue that the values of fluid behavior index N in this study were not significantly different than 1. However, blocking laws as derived from Rabinowitsch–Mooney equation assume fluid transport phenomenon in capillaries. If we consider flow in the membrane capillary (e.g. as for 0.8 μm pore diameter used in this study), we must consider such a transport phenomenon as flow in a microchannel where the effect of fluid behavior index in a microscale channel can be significantly larger than that in the macrochannel. Hadigol and co-workers [25] did a numerical analysis of mixed electroosmotic-pressure driven flow of power law fluids in a microchannel of 20 μm \times 92.8 μm (height \times length) and showed that the volumetric flow rate depends heavily on N when other operational conditions (i.e. zeta potential, Debye length, external electric potential, and channel height) are set constant. Fluid with N values of 0.93 and 1.03 were reported to give around 160 and 80% volumetric flow, respectively, in comparison to that of a fluid with N value of 1.

3.2. Size measurements of the feed solutions

Particle size distribution analyses based on volume percentage of the two feed solutions used is presented

in Fig. 5. Kaolin displayed a broad range of particle sizes from 0.1 to 12 μm , with two distinctive peaks around 5 and 11 μm (manufacturer specification was 0.1–4 μm). The nominal size of TiO_2 reported by the manufacturer is around 21 nm, however, the size measurement revealed existence of larger TiO_2 particles with three distinct peaks observed at size ranges of 0.05–0.06, 0.2–0.3, and 0.5–0.6 μm . Such a phenomenon is common for TiO_2 dispersions due to agglomeration, especially in high concentrations [26]. The standard deviations (dashed lines in Fig. 5) suggest that kaolin agglomerates were more stable and less prone to deformation as the deviations observed were small. In contrast, TiO_2 particles were more susceptible to change where results showed that the amount of larger agglomerates gradually decreased (i.e. reduction in peak), and where the amount of smaller particles increased (i.e. increase in peak) as repetition analysis with the same samples were performed. The impact of the changes in particle properties over time should be considered when determining the fouling behavior of such feed solutions. Nonetheless, fractions of particle smaller than the pore size of the membrane exist opening the possibility to observe pore-type fouling phenomenon. Size measurement for CMC was not conducted since it is soluble in water with the reported average molecular weight of 90 kDa.

3.3. Microfiltration of kaolin and TiO_2

Fig. 6 presents the results of filtration experiments at different fluxes and concentrations of kaolin and

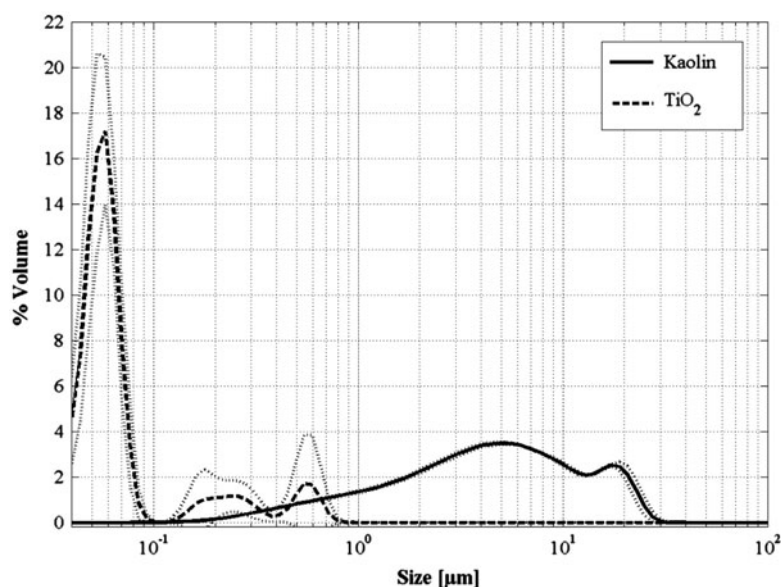


Fig. 5. Particle size distributions of feed solutions (the dotted lines represent standard deviation of the measurements).

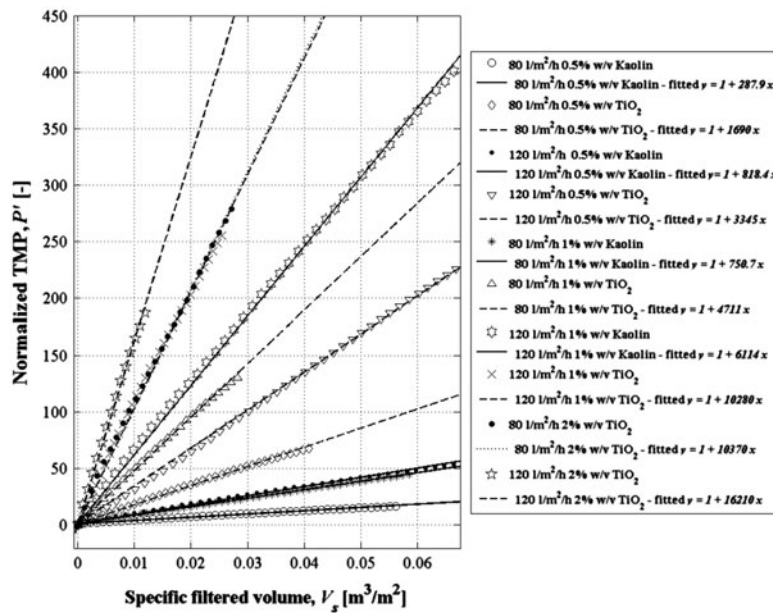


Fig. 6. Fitting results for filtration experiments of kaolin and TiO_2 .

TiO_2 . Judging from the data plot, cake filtration appears to be the dominant fouling mechanism. For fitting the data, the expression for cake filtration in Eq. (22) can be simplified by normalizing the trans-membrane pressure (TMP) P over initial TMP P_0 and filtered volume V over initial active membrane area A_0 . This gives the following equation;

$$P' = 1 + k_{CF} \cdot V_s \quad (24)$$

where $P'[-]$ is the normalized TMP, $V_s[\text{m}^3/\text{m}^2]$ is the specific filtered volume, and the blocking constant k_{CF} is thus modified to $c_f \cdot \hat{R}_c/R_m[\text{m}^{-1}]$. A similar formulation was reported by Huang et al. [21] with a slight modification as the expression was normalized with respect to specific flux (J'_s) instead of normalized TMP as proposed in this study. For the same experimental conditions, TiO_2 contributed to a higher hydraulic resistance in comparison to kaolin, as represented by steeper slopes of the lines in Fig. 6. This can be attributed to the differences in particle size distribution of the two materials. From the analysis shown in Fig. 5, the TiO_2 solution was dominated by smaller particles which results in lower cake porosities compared to that of larger particles, as in the case of the kaolin solution.

The sedimentation effect is insignificant in the case of TiO_2 since the filtration rate ($2.22\text{--}3.33 \times 10^{-5} \text{ m/s}$, corresponding to flux of $80\text{--}120 \text{ l/m}^2/\text{h}$) is much

higher than the settling velocity of TiO_2 ($4.40\text{--}6.32 \times 10^{-9} \text{ m/s}$, calculated using Stokes's formula for the smallest and the largest sizes). However, sedimentation effect may be significant for kaolin particles larger than $5 \mu\text{m}$ (corresponding to $\sim 30\%$ of the total particle volume) since the settling velocity is higher than the filtration rate. Both the measured and fitted data confirm that in the range of concentrations used in this study, the blocking law based on cake filtration predicts the linearity of the TMP increase correctly for both Newtonian and non-Newtonian fluids, as also revealed in [23]. However, the concentration of solids plays an important role in emphasizing non-Newtonian fluid characteristics. The continuity of the fluid rheology in this case was questionable since most of the materials were retained by the membrane in the cake structure. This was confirmed by rheology tests of the filtrate that showed Newtonian fluid characteristic, which emphasizes the question whether the blocking laws for non-Newtonian fluids are really applicable, or important to that matter, even though the correlations of the data in Fig. 6 are very good (R^2 values between 0.99 and 1).

3.4. Microfiltration of CMC

Fig. 7 plots the filtration data and the model fitting results of CMC. The non-linear nature of the data plot suggests a different filtration behavior of CMC than that of kaolin and TiO_2 . The data was fitted by the sets of blocking laws equations for both Newtonian and

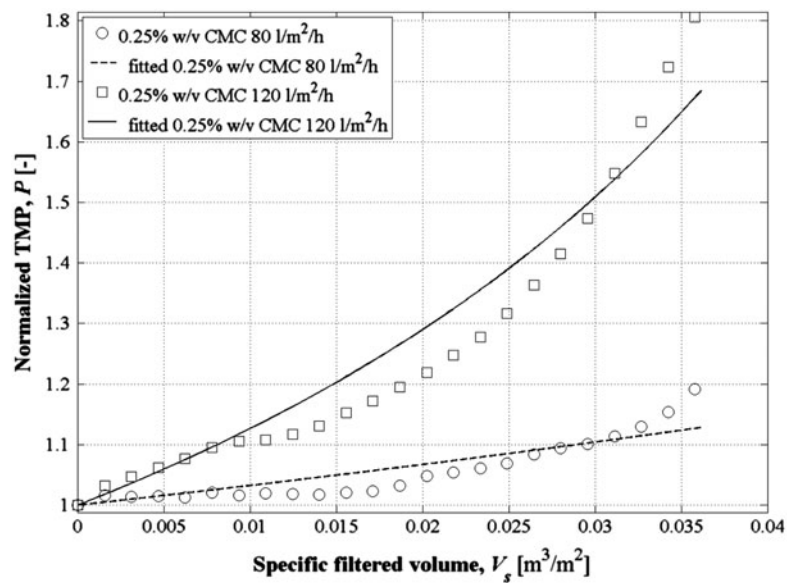


Fig. 7. Fitting results for filtration experiments of CMC.

non-Newtonian fluid (Table 2). Although the R^2 values were reasonably low (0.80 and 0.93 for 80 and 120 l/m²/h, respectively), interestingly the best fits came from the set of equations of blocking laws for non-Newtonian fluid with complete blocking prevailing as the dominant fouling mechanism. The structure of CMC was reported to be fibrous [27,28] and the presence of low salt concentration and high background pH in this study most likely would not coil the structure. As in the case of kaolin and TiO₂, rheology tests of the filtrate from microfiltration of CMC also showed Newtonian fluid behavior, which suggests retention of dissolved material by the membrane. With this knowledge, cake filtration might provide the better explanation of such a fouling phenomenon except that the nature of the cake material of CMC is different than that of kaolin or TiO₂. Fibrous materials might have a higher degree of freedom to be rearranged or consolidated, thus the case shown here might be the case of cake compression or consolidation of CMC material.

Nonetheless, the result of rheology tests of the filtrate leads to further questioning the applicability of such a model in the presence of interaction between the membrane and the fluid/medium given that the fluid characteristic through the pores of the membrane changes. In literature, the works on non-Newtonian fluid filtration modeling using blocking laws seldom reported the rheology of the filtrate, which is actually an important aspect in confirming the applicability of the models. The observations from this study as

presented in this manuscript cannot really confirm the applicability of blocking laws for constant flux filtration of non-Newtonian fluid. Tien and Ramarao [29] questioned the validity of blocking laws in general and suggested that the usual resistance-in-series approach might be sufficient to elucidate the membrane fouling phenomenon. Shirato et al. [23] were among the pioneers in using blocking laws for constant flux non-Newtonian fluid filtration, and in that particular work they used an approach similar to that suggested by Tien and Ramarao.

4. Conclusions

This paper deals with deriving the classical blocking laws for constant flux membrane filtration that incorporates the rheology aspects of the fluid being filtered. The theory clearly shows that rheology needs to be considered in the application of the model. However, the result of filtration experiments in this study showed rheological inconsistency between the feed solution and the filtrate, i.e. Newtonian fluid behavior of the filtrate. This finding suggests that the application of the blocking laws for constant flux non-Newtonian fluid filtration could not be thoroughly confirmed. Nonetheless, the work presented here provides a starting point for further study of non-Newtonian fluid filtration. Alternatively, development of new models or approaches is therefore probably more appropriate in defining the fouling behavior for such conditions.

Acknowledgment

The authors would like to thank Ardi Hartono PhD at the Chemical Engineering Department NTNU for the assistance provided during rheology tests and the Research Council of Norway (NFR) for funding the research.

References

- [1] R.P. Chhabra, *Bubbles, Drops, and Particles in Non-Newtonian Fluids*, 2nd ed., CRC Press, Boca Raton, FL, 2006.
- [2] N.P. Cheremisinoff, *Encyclopedia of Fluid Mechanics*, Book Division, Gulf Pub. Co., Houston, TX, 1986.
- [3] J.F. Steffe, *Rheological Methods in Food Process Engineering*, 2nd ed., Freeman Press, East Lansing, MI, 1996.
- [4] M. Mori, I. Seyssiecq, N. Roche, Rheological measurements of sewage sludge for various solids concentrations and geometry, *Process Biochem.* 41 (2006) 1656–1662.
- [5] M. Mori, J. Isaac, I. Seyssiecq, N. Roche, Effect of measuring geometries and of exocellular polymeric substances on the rheological behaviour of sewage sludge, *Chem. Eng. Res. Des.* 86 (2008) 554–559.
- [6] B. Seyssiecq, B. Marrot, D. Djerroud, N. Roche, In situ triphasic rheological characterisation of activated sludge, in an aerated bioreactor, *Chem. Eng. J.* 142 (2008) 40–47.
- [7] H. Reihanian, C.R. Robertson, A.S. Michaels, Mechanisms of polarization and fouling of ultrafiltration membranes by proteins, *J. Membr. Sci.* 16 (1983) 237–258.
- [8] J.G. Wijmans, S. Nakao, C.A. Smolders, Flux limitation in ultrafiltration: Osmotic pressure model and gel layer model, *J. Membr. Sci.* 20 (1984) 115–124.
- [9] M.W. Chudacek, A.G. Fane, The dynamics of polarisation in unstirred and stirred ultrafiltration, *J. Membr. Sci.* 21 (1984) 145–160.
- [10] C. Tien, B.V. Ramarao, On analysis of cake formation and growth in cake filtration, *J. Chin. Inst. Chem. Eng.* 37 (2006) 81–94.
- [11] W.M. Lu, C.C. Lai, K.J. Hwang, Constant pressure filtration of submicron particles, *Sep. Technol.* 5 (1995) 45–53.
- [12] J. Hermia, Constant pressure blocking filtration laws - Application to power-law non-Newtonian fluids, *Trans. Inst. Chem. Eng.* 60 (1982) 183–187.
- [13] M. Shirato, T. Aragaki, E. Iritani, M. Wakimoto, S. Fujiyoshi, S. Nanda, Constant pressure filtration of power-law non-Newtonian fluids, *J. Chem. Eng. Jpn.* 10 (1977) 54–60.
- [14] V. Chen, A.G. Fane, S. Madaeni, I.G. Wenten, Particle deposition during membrane filtration of colloids: Transition between concentration polarization and cake formation, *J. Membr. Sci.* 125 (1997) 109–122.
- [15] C.-C. Ho, A.L. Zydney, A Combined Pore Blockage and Cake Filtration Model for Protein Fouling during Microfiltration, *J. Colloid Interface Sci.* 232 (2000) 389–399.
- [16] K.J. Hwang, C.Y. Liao, K.L. Tung, Analysis of particle fouling during microfiltration by use of blocking models, *J. Membr. Sci.* 287 (2007) 287–293.
- [17] M. Shirato, T. Aragaki, E. Iritani, Analysis of constant pressure filtration of power law non-Newtonian fluids, *J. Chem. Eng. Jpn.* 13 (1980) 61–66.
- [18] M. Hlavacek, F. Bouchet, Constant flowrate blocking laws and an example of their application to dead-end microfiltration of protein solutions, *J. Membr. Sci.* 82 (1993) 285–296.
- [19] M. Shirato, T. Aragaki, E. Iritani, Blocking filtration laws for filtration of power-law non-Newtonian fluids, *J. Chem. Eng. Jpn.* 12 (1979) 162–164.
- [20] S. Chellam, W. Xu, Blocking laws analysis of dead-end constant flux microfiltration of compressible cakes, *J. Colloid Interface Sci.* 301 (2006) 248–257.
- [21] H. Huang, T.A. Young, J.G. Jacangelo, Unified membrane fouling index for low pressure membrane filtration of natural waters: Principles and methodology, *Environ. Sci. Technol.* 42 (2008) 714–720.
- [22] Y. Bessiere, N. Abidine, P. Bacchin, Low fouling conditions in dead-end filtration: Evidence for a critical filtered volume and interpretation using critical osmotic pressure, *J. Membr. Sci.* 264 (2005) 37–47.
- [23] M. Shirato, T. Aragaki, E. Iritani, T. Funahashi, Constant rate and variable pressure-variable rate filtration of power law non-Newtonian fluids, *J. Chem. Eng. Jpn.* 13 (1980) 473–478.
- [24] M. Santillán, F. Membrives, N. Quaranta, A. Boccacini, Characterization of TiO₂ nanoparticle suspensions for electrophoretic deposition, *J. Nanopart. Res.* 10 (2008) 787–793.
- [25] M. Hadigol, R. Nosrati, M. Raisee, Numerical analysis of mixed electroosmotic/pressure driven flow of power-law fluids in microchannels and micropumps, *Colloids Surf. A* 374 (2011) 142–153.
- [26] G. Brunelli, S. Pojana, A. Callegaro, Marcomini, Agglomeration and sedimentation of titanium dioxide nanoparticles (n-TiO₂) in synthetic and real waters, *J. Nanopart. Res.* 15(6) (2013) 1–10.
- [27] J. Elliot, A. Ganz, Some rheological properties of sodium carboxymethylcellulose solutions and gels, *Rheol. Acta* 13 (1974) 670–674.
- [28] B. Khaled, B. Abdelbaki, Rheological and electrokinetic properties of carboxymethylcellulose-water dispersions in the presence of salts, *Int. J. Phys. Sci.* 7 (2012) 1790–1798.
- [29] C. Tien, B.V. Ramarao, Revisiting the laws of filtration: An assessment of their use in identifying particle retention mechanisms in filtration, *J. Membr. Sci.* 383 (2011) 17–25.